Investigation of Plastic Freeformed, Open-Pored Structures with Regard to Producibility, Reproducibility and Liquid Permeability

Andre Hirsch[1(✉)], Christian Dalmer[2], and Elmar Moritzer[1]

[1] Kunststofftechnik Paderborn (KTP), Direct Manufacturing Research Center (DMRC), Paderborn University, 33098 Paderborn, Germany
andre.hirsch@ktp.upb.de
[2] Paderborn University, Warburger Str. 100, 33098 Paderborn, Germany

Abstract. The Arburg Plastic Freeforming (APF) is an additive manufacturing process which allows the production of three-dimensional thermoplastic components in layers. The components are produced by depositing fine, molten plastic droplets. The main advantage of the APF is the open-parameter control of the associated machine system. Thus, the process parameters can be optimized for individual applications.

A special and new application of the APF is the production of interconnecting porous structures. As this is a novel approach with this manufacturing process, the general producibility and reproducibility must first be proven. Therefore, the relevant process parameters with an influence on the open-pored structures are identified. The volume of the individual plastic droplets, the distance between the droplets and the layer thickness are the three decisive influencing factors. With the use of analysis methods, the free spaces created in the structure are described by a uniformly constructed, interconnected pore structure. This means that the pores are interconnected in three dimensions.

Reproducibility is evaluated by repeated production and thru the changed conditions during the manufacturing process. In addition, the multiplication and a change of geometry are evaluated in such a way that there is no influence on the pore size. Irregularities when depositing the first layer are caused by unevenness of the building platform. A suitable test arrangement is set up to determine the liquid permeability. A characteristic value is determined to describe the permeability to liquids.

Keywords: Arburg Plastic Freeforming · Porous plastic structures · Producibility · Liquid permeability

1 Introduction

The Arburg Plastic Freeforming (APF) is an additive manufacturing process that allows three-dimensional, thermoplastic components to be produced layer by layer. The components are generated by depositing fine, molten plastic droplets. One of the main advantages of the APF process is the open machine control. Thus, the process parameters can be adapted and optimized for individual applications. In addition, due to

the open-parameter control, it is possible to process own materials on the corresponding machine system Freeformer.

The objective of this paper is to investigate the general producibility of open-pored structures using the APF process. Furthermore, influences on the reproducibility of the manufacturing process are to be identified and their effects are to be shown. With regard to possible fields of application, a correlation between the manufactured structures and their fluid permeability shall be investigated.

2 State of the Art

2.1 Arburg Plastic Freeforming (APF)

The Arburg Plastic Freeforming is characterized in particular by the processing of standard plastic granules as well as by the production of components out of very fine molten thermoplastic droplets. The associated machine system for this technology is the Freeformer from Arburg GmbH & Co KG. Its most important machine components are shown in Fig. 1. The raw material, a qualified standard thermoplastic granule, is fed via a hopper. In the material preparation unit, the granulate is molten with a screw as in the injection molding process. The molten material is then pressed into the material reservoir. Here, a piezo actuator performs a pulsed nozzle closure. The nozzle moves up and down, producing almost 250 droplets per second. The movement of the building platform, for the precise positioning of the discharged droplets in the x- and y-direction, is realized by two linear motors. After the completion of a layer the platform is lowered by one-layer thickness in z-direction, using a spindle drive [1–3].
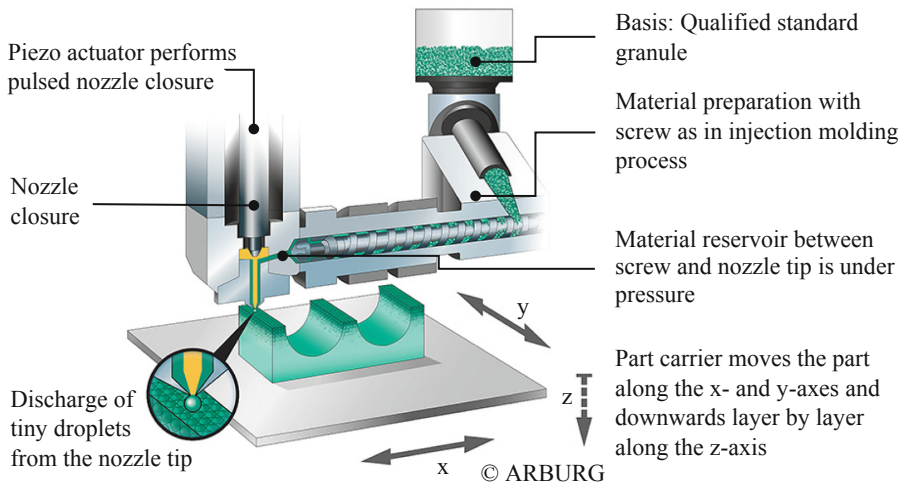

Fig. 1. Schematic setup of the Freeformer [1]

In the literature there is a large number of publications by the Arburg company with process descriptions, the advantages of the technology, the available materials and application examples [2–5]. In [6–8] the resulting mechanical properties of APF components were investigated and optimized. Furthermore, new approaches for the production of two-component (hard-soft) parts with interlocking interfaces as well as for the suitability of the APF process for the processing of Metal-Injection-Molding granules are found in the literature [9, 10].

2.2   Porosity

Porosity is a structural characteristic of a component and describes the existence of pores. Pores are classified into open and closed structures. Closed pores are located within a component. They are completely enclosed within the component so that there is no connection to the environment. Open pores are further divided into blind and continuous pores (see Fig. 2). Blind pores have one connection to the environment, whereas continuous pores have at least two connections to the environment. When a medium (liquid or gas) flows through a component, the number and geometry of the pores contributes to the degree of permeability [11, 12].
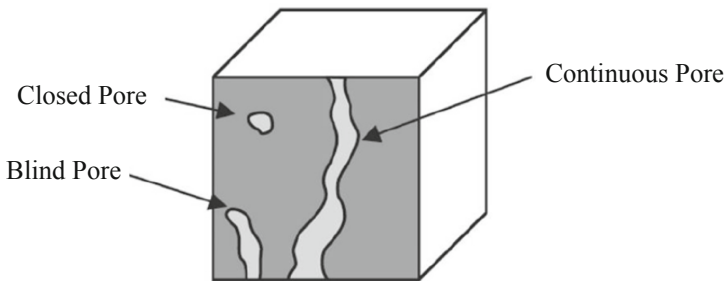

Fig. 2. Division of the pore types into open, closed and blind pores

A further classification is based on the size of the pore size. The following size ranges are differentiated by diameter:

- Micropores: <2 nm
- Mesopores: 2 to 50 nm
- Macropores: >50 nm (0.05 μm)

The porosity ϵ of a material is determined using Eq. (1) and describes the percentage of free volume:

$$\epsilon = 1 - \frac{\rho_{Specimen}}{\rho_{Reference}} \qquad (1)$$

$\rho_{Specimen}$:   Density of the porous specimen
$\rho_{Reference}$:   Density of the non-porous material (Reference)

2.3 Applications of Open-Pored Structures

An exemplary application of open-pored structures is filtration, where a filter is able to serve different purposes. If two media are separated from each other, this is called filtration or separation. The filter retains particles that are larger than the minimum pore diameter. Furthermore, it is possible to mix different gases with each other (dispersion) by using branches and a multi-layer structure within the filter element [11].

2.4 Liquid Permeability

The permeability is a material constant and describes the flow-through capability of a porous material. Permeability provides information about the volume of a permeant (gas or liquid) that penetrates a barrier of a given thickness and area per unit of time, provided that there is a partial pressure difference at the interfaces of the barrier [13]. The following three basic equations are used for mathematical description:

- Continuity equation (conservation of mass)
- Law of Darcy (conservation of momentum)
- Thermodynamic equation of state

The continuity equation implies that the sum of all masses flowing in and out is equal to the mass change of the sample. Darcy's law specifies the relationship between the flow velocity within the pores and the potential gradient, considering the height and acceleration due to gravity. With the help of the thermodynamic equation of state, the dependence of the density of the permeant on the pressure, at constant temperature, is included [14]. By combining the basic equations, Eq. (2) defines the permeability (K) with the unit m^2:

$$K = \frac{\dot{V} \cdot \eta \cdot L}{\rho \cdot g \cdot A \cdot \Delta h} = \frac{k_f \cdot \eta}{\rho \cdot g} \qquad (2)$$

$\dot{V}$:   Volume flow
η: Dynamic viscosity of the permeant
L: Length of the barrier
ρ: Density of the permeant
g: Acceleration of gravity
A: Cross-sectional area of the barrier through which flow occurs
Δh: Difference in height between inlet and outlet
k_f: Permeability coefficient

As can be seen from Eq. (2), permeability can be expressed by a second definition, the coefficient of permeability (k_f), with the unit m/s. The formulaic relationship is described in DIN 18130-1 and is given in Eq. (3) below:

$$k_f = \frac{\dot{V} \cdot L \cdot \rho \cdot g}{A \cdot \Delta p} \tag{3}$$

Δp: Pressure difference between inlet and outlet

Once the permeability coefficient has been calculated, the permeability of water can be classified according to DIN 18130-1 (see Table 1).

Table 1. Classification of permeability according to DIN 18130-1

Description	Permeability coefficient k_f [m/s]
Very highly permeable	$>10^{-2}$
Highly permeable	10^{-2} bis 10^{-4}
Permeable	10^{-4} bis 10^{-6}
Low permeability	10^{-6} bis 10^{-8}
Very low permeability	10^{-8} bis 10^{-9}
Almost completely impermeable to water	$<10^{-9}$

3   Producibility of Open-Pored Structures

The beginning of this study is based on a randomly produced component (see Fig. 3, left) from the qualification of the material polypropylene (PP) Moplen HP 500 N for the APF process. The aim of such material qualification is to determine all relevant process parameters so that components with the required mechanical and visual properties can be produced. During this process parameter optimization, a porous, translucent structure was created by changing the layer thickness (see Fig. 3, right).
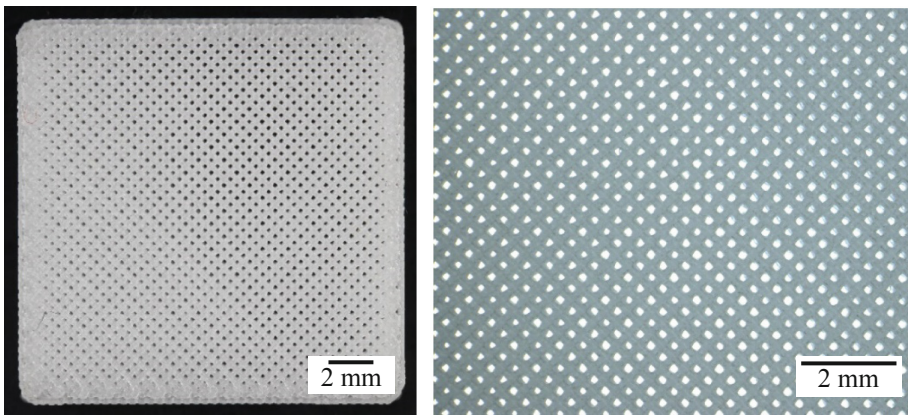

Fig. 3. Initial specimen in full size view (left) and with enlargement (right)

The porous structure looked very homogeneous, which lead to the idea of carrying out detailed investigations. However, due to the unavoidable warpage of the parts caused by the semi-crystalline PP, the following tests were not carried out with PP, but with the already qualified material ABS Terluran GP 35.

3.1   Variation of the Layer Thickness (LT)

Initially, the aim was to produce an open-pored structure using the material ABS Terluran GP35 by varying the layer thickness (LT). For the following investigations all parameters, except LT, remain unchanged. The layer thickness is increased from 0.15 mm in steps of one hundredth of a millimeter. The evaluation of the measurement results is shown below in Fig. 4 and 5.
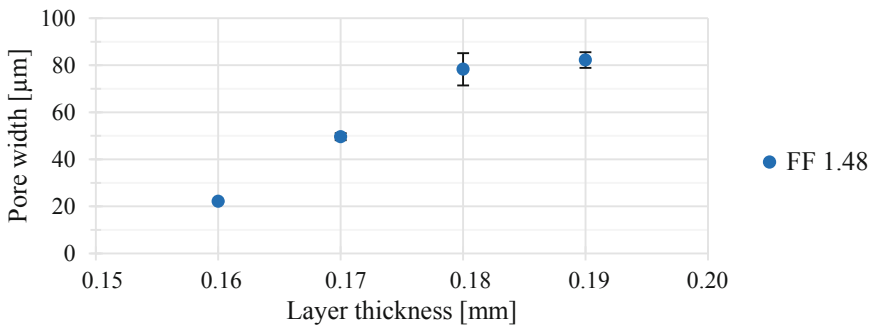

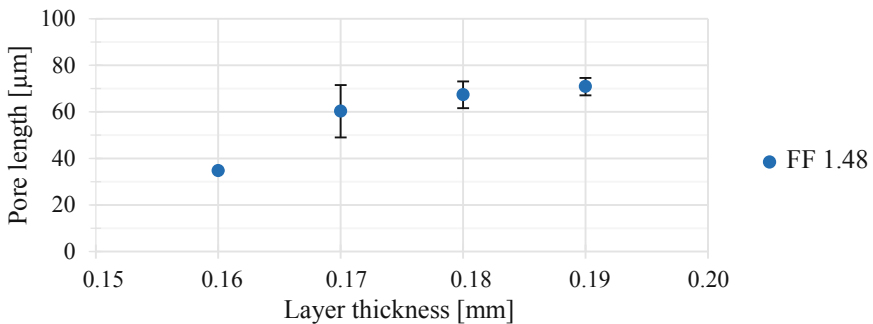**Fig. 4.** Pore widths with different LT

Fig. 5. Pore lengths with different LT

   The diagrams in Fig. 4 and 5 show that the size of the pores increases with increasing layer thicknesses. Pore openings with widths between 22 and 82 μm are produced. The lengths are in a range of 34 to 71 μm. This corresponds to the order of magnitude of macropores.

Computer tomography (CT) scans shown in Fig. 6 were taken from the specimen produced with LT = 0.18 mm and FF = 1.48. The CT images show a rectangular structure of the cylindrical specimen. This change in geometry is the result of the CT evaluation, in which a rectangular ROI ("Region of Interest") was cut out of the overall image.
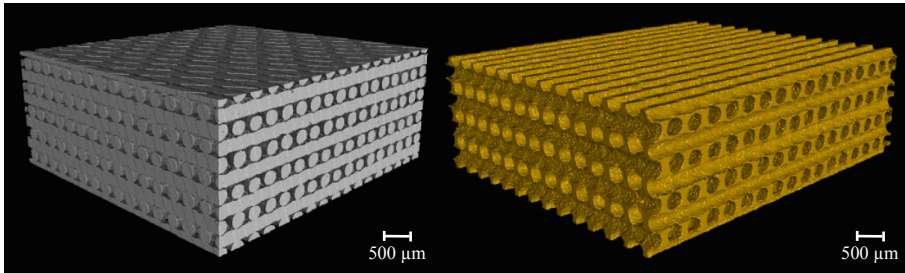

Fig. 6. CT scan of the porous structure (left) and its inversion to show the pore volume (right)

The CT scan of the sample shows the principal composition of the porous structure. The inversion of the volume allows not only the continuous openings in z-direction to be detected, but also a connection of the pores in transverse direction. There is an interconnection in all directions in the volume. Because of this, it is not possible to differentiate between individual pores within the produced samples, instead there is a continuous free space. If terms are used in the following to describe the pore size or geometry, they are related to the pore openings visible on the surface.

3.2   Variation of the Form Factor (FF)

The form factor is used to vary the distance between the single droplets and between the droplet chains (see Fig. 7) [15]. This process parameter is defined by the ratio of the width (W) to the height (H) of the individual droplets (W/H-ratio). Consequently, the FF influences the porosity and filling of the components. For the following investigations, only the parameter FF is varied. According to theory, the distance between the droplets is reduced as the FF decreases. The basic setting for the FF is 1.48 for the
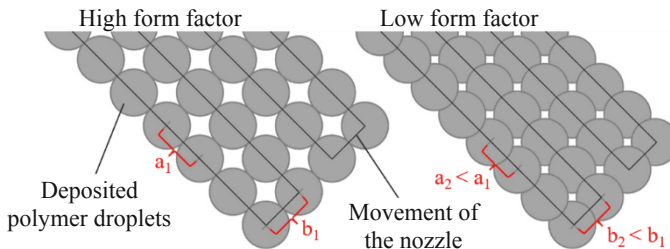

Fig. 7. Schematic description of the process parameter form factor [15]

current material and results a fully filled component. The variation of the parameter is started with a rounded value of 1.50. The factor is then increased in tenth steps. Subsequently, the created samples are visually examined and categorized.

The porous structures produced by variation of the FF do not differ visually from the samples produced by variation of the LT. The decreasing stability of the component with increasing FF is also noticeable in this case. At an FF of 2.50, individual strands of the last layer built stand out from the rest of the component.

When evaluating the pore geometry, a correlation between pore length/width and an increasing form factor can be observed (see Fig. 8 and 9). To describe this correlation, the calculation of the correlation coefficient r according to Bravais-Pearson is used. The correlation coefficient ranges between −1 and 1 and indicates the direction and intensity of a linear correlation. If r = 1 (r = −1) there is a strong positive (negative) linear correlation. If r = 0 there is no linear correlation. Due to the resulting values of r = 0.999 for the pore width and r = 0.995 for the pore length, a positive linear correlation is assumed.
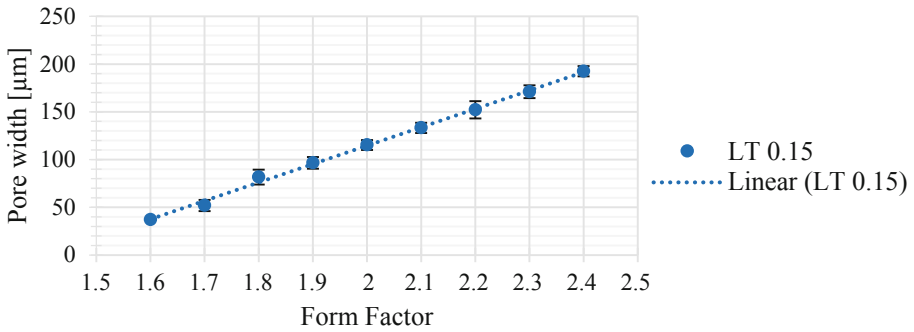

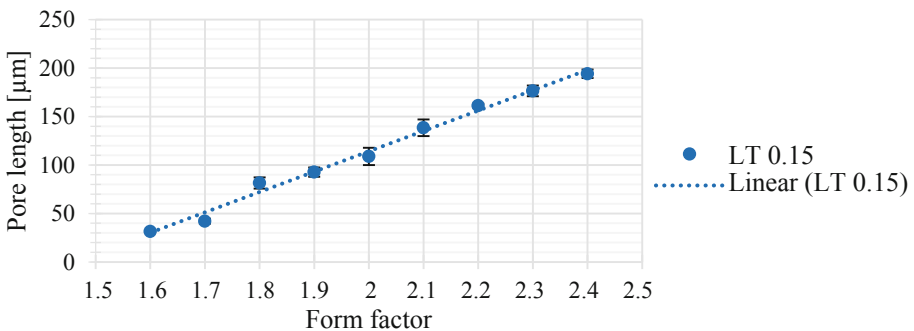**Fig. 8.** Pore widths with different FF

Fig. 9. Pore lengths with different FF

The variation of the FF results in porous structures with pore widths in a range of 37 to 192 µm. The pore lengths cover a range between 32 and 194 µm. The pore geometries can again be assigned to the macropores. In comparison to the variation of LT, significantly larger pores can be created with the variation of the FF. The FF can be adjusted in hundredths of a step during part preparation (slicing). In combination with a linear relationship between the pore size and the FF, it is possible to adjust the pore sizes almost continuously within the determined ranges.

3.3   Variation of the Discharge Level (DL)

The discharge level describes the mass discharge of material from the dosing volume through the nozzle. Accordingly, the setting of the discharge level results in the respective volume of the droplets as well as the droplet size. The discharge level is set as a percentage and is controlled by the travel of the screw during the generation of droplets. In order to investigate the influence of the discharge level on the building process, it is first doubled. According to the basic settings, the doubling of the discharge level corresponds to an increase from 35 to 70%. Since this adjustment changes the droplet geometry, a new LT must be defined. To do this, the droplet strand is discharged into the build chamber without being deposited on the building platform and then measured by means of microscopy (see Fig. 10).
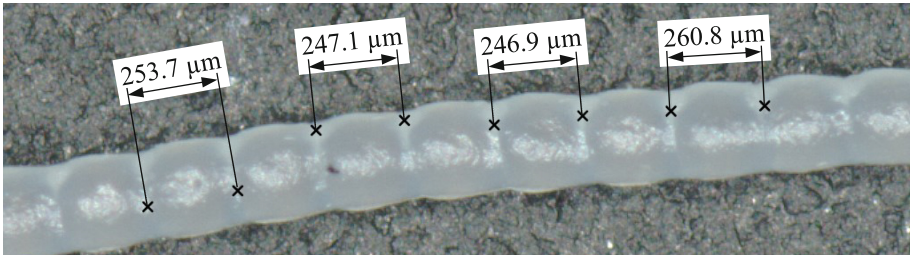

Fig. 10. Droplet strand with DL of 70%

Rounding results in an average droplet length of 0.25 mm. This value is used for an initial setting of the LT. Subsequently, the procedure of varying the FF is to be applied so that a parameter range can be identified to create a porous structure. For the measured values presented in Fig. 11 and 12, the lowest coefficient of correlation is r = 0.99. As a result, a linear correlation between the form factor and the pore size is still established.

An increase in the pore size range can be achieved by doubling the discharge level. The pore widths are in a range between 63 and 280 µm and the pore lengths between 76 and 282 µm. Compared to the previously produced samples, larger pores can be produced by increasing the discharge. An extension of the pore size range in negative direction is not possible.
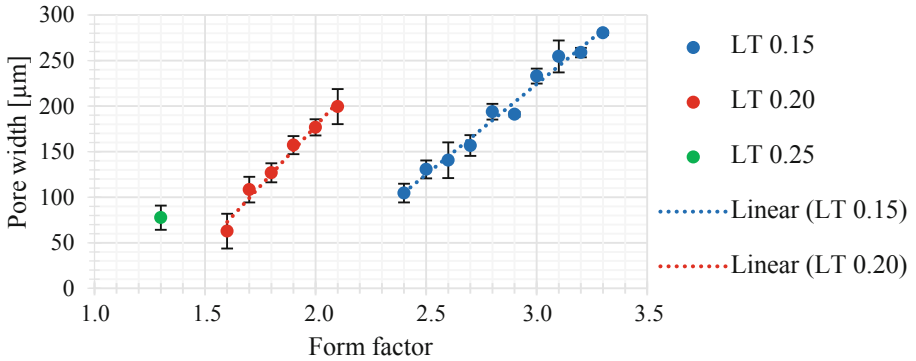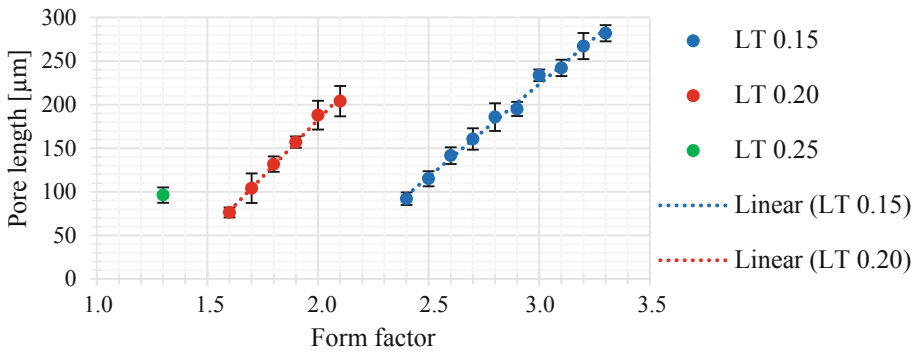
Fig. 11. Pore widths for DL of 70%

Fig. 12. Pore lengths for DL of 70%

To determine the maximum possible pore size that can be produced with APF, the discharge is increased further. The original value of 35% is tripled to 105%. To determine the initial layer thickness, the measurement of the droplet strand yields an average droplet length of 300 μm. Accordingly, the variation of the FF should be started at LT of 0.30 mm. The results of the investigations are shown in Fig. 13 and 14.

The evaluation of the measurement results again shows that the range for the production of a porous structure with LT of 0.15 mm has increased considerably. The pore size range is so large that the achievable sizes are also covered by the layer thickness of 0.20 mm and 0.25 mm. The pore widths are in the range of 84 to 466 μm and the pore lengths in the range of 58 to 440 μm. This is a further extension of the pore size range in the positive direction. It should be noted that the droplets are in a deformed state. This deformation results from the forced discharge of more material in a constant time interval. A further increase in the degree of deformation does not allow reproducible categorization or measurement of the pore geometry. Therefore, no further increase of the discharge level is performed.
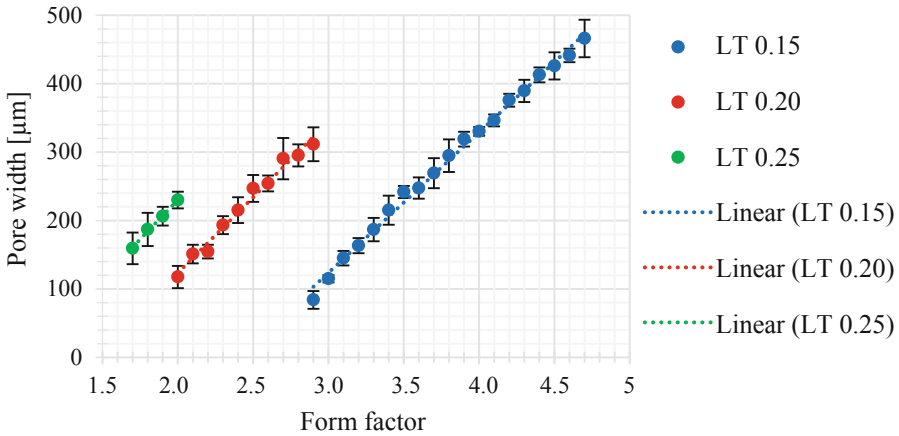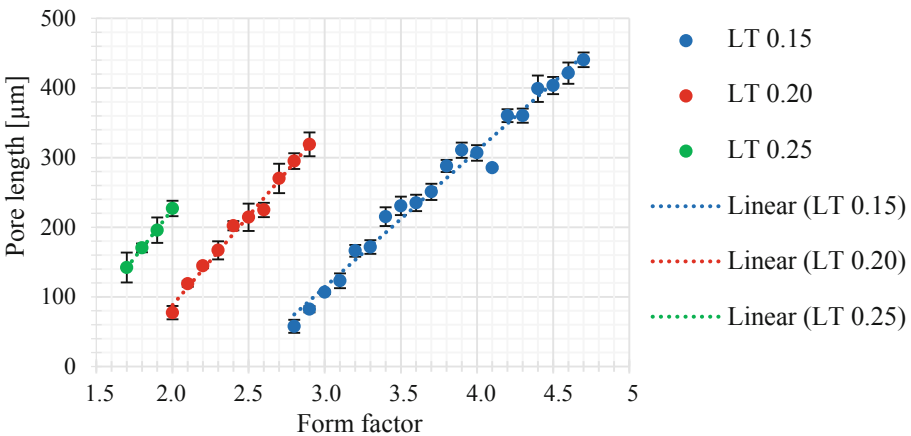
Fig. 13. Pore widths for DL of 105%

Fig. 14. Pore length for DL of 105%

4 Reproducibility of Open-Pored Structures

In this section, the reproducibility of the porous structures in the APF process is investigated. The influence of the position on the building platform and the multiplication of the components is considered. With the aim of investigating the influences on a porous structure, the FF is increased from the value 1.48 to 2.00. This setting shows a uniform pore structure on the surface.

4.1   Positioning on the Building Platform

Unevenness is indicated by an inconsistent depositing position of the plastic droplets in the z-direction. Furthermore, it is assumed that a changed distance between the discharge nozzle and the building platform (z-coordinate) leads to a different pressing of the first layer. To detect the degree of contact pressure, the strand width of the lined-up plastic droplets is used as a measured variable. If the distance between the discharge nozzle and the building platform decreases, the strands are pressed onto the building platform with increased force. It should be possible to determine the result by means of a widened strand geometry.

To investigate the evenness, 13 different positions are defined for the build-up of test specimens (see Fig. 15). The coordinates shown indicate the respective center point of the element to be built. Three building jobs are built, so that each test specimen is available for examination in three versions. It should be noted that only one test specimen per building job is produced, as the influence of a multiplication of the building job has not yet been investigated. As with the measurement of the pore geometry, the widths of five strands per sample are recorded and the mean value is calculated (see Fig. 15).
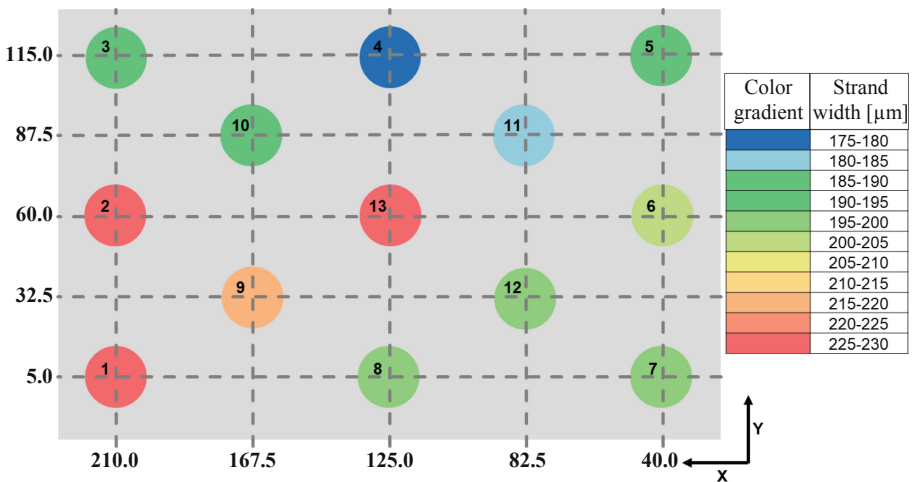

Fig. 15. Averaged strand widths depending on the positioning on the building platform, measured on the platform side and evaluated with a color scale

The assumption regarding unevenness on the building platform can thus be confirmed. The averaged strand widths at the different positions vary in a range between 176 and 228 μm. In addition to the strand width, the manufactured test specimens are used to assess the reproducibility of the pore sizes at the nozzle side. For the pore width an average value of 120 μm with a standard deviation of 4.8 μm is available. The lengths of the square pore geometry are given including the standard deviations, with a nominal value of 115 μm and a tolerance of ±10 μm.

4.2   Multiplication of the Test Specimen

Previously, a maximum of one test specimen was produced per building job. In this section the influence of a multiplication of the test specimen is examined. When building several components simultaneously within one building job, a layer is first built for all components before the following layer is deposited. This results in a longer layer time. In addition, the nozzle is not permanently located above the part to be built up, as is the case in the production of only one component. This eliminates the additional heating effect of the heat radiated by the nozzle.

To investigate the above-mentioned influences on the pore size, five test specimens are built up simultaneously in three runs. The tolerance range of 115 ± 10 µm previously determined in the investigations serves as a reference. Due to the assumption of a square pore geometry, the pore length is not shown in the following evaluations. The determined pore widths are in a range between 106 and 115 µm (see Fig. 16) and the pore lengths between 119 and 125 µm. Accordingly, the specified tolerance range is maintained. The multiplication of a component has no influence on the size of the generated pore geometries.
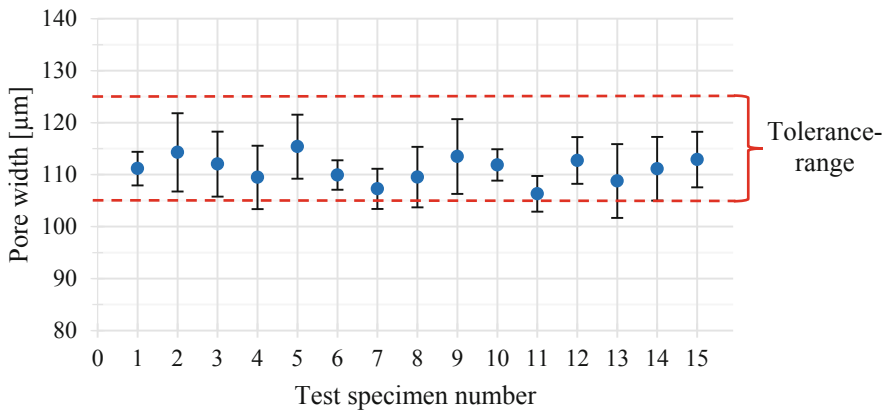

Fig. 16. Determined pore widths when multiplying a building job by the factor 5, measured at the nozzle side

5   Liquid Permeability of Open Porous Structures

Based on the results from macroscopy, components with macropores are to be examined. Macropores correspond to the largest area within the pore classification. Accordingly, medium to high permeabilities are expected, so that a stationary measurement with a liquid is to be carried out. The following conditions must be observed [14]:

1. Cylindrical or square test pieces shall be used
2. No reactions with the pore wall take place
3. The flow is single-phase (homogeneous liquid)
4. The flow is stationary
5. The flow is formed

Condition (1) is ensured by the possibility of a freely selectable geometry by means of APF during the production of the test specimens. Demineralized water is used to ensure compliance with conditions (2) and (3). Aspects (4), (5) shall be considered in the design of the test setup and the performance of the test. A possible setup is shown in Fig. 17.
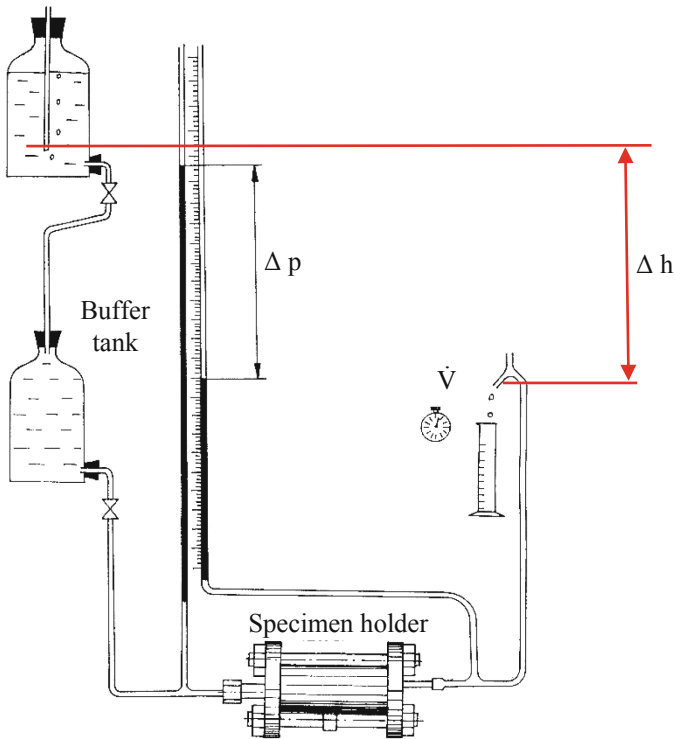

Fig. 17. Experimental setup for a stationary measurement of liquid permeability [14]

The basic principle of the measurement is to measure the resulting volume flow, which flows through a sample under the application of a constant pressure. The volume flow changes depending on the resistance of the sample to the medium flowing through it.

The specimen holder (see Fig. 18) has the function of clamping the specimens to be tested and ensuring that the fluid flows through them. The liquid flow passes through the inlet (3) on the upper side, through the porous structure and then into the outlet on the lower side.
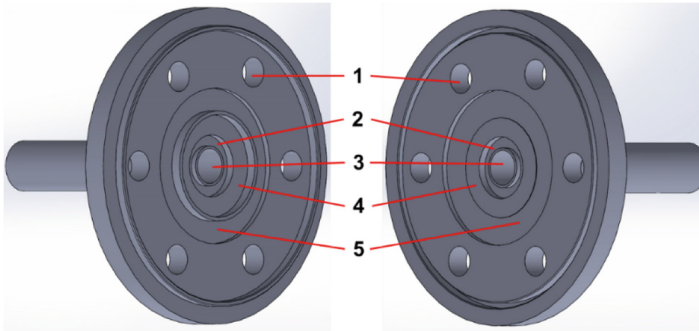
Fig. 18. Upper side (left) and lower side (right) of the specimen holder. 1: Through-bore, 2: Groove for inner O-rings, 3: Inlet and outlet of the test liquid, 4: Specimen contact area, 5: Groove for outer O-ring

The results of the tests are divided for evaluation. First, the evaluation of the structures with DL of 35% is shown (see Fig. 19). With increasing FF as well as with increasing LT linear relationships between the mass flow rate and the parameters can be seen. The correlation coefficients are above r = 0.98. These correlations simultaneously describe an increase in volume flow with increasing pore openings within a parameter variation.
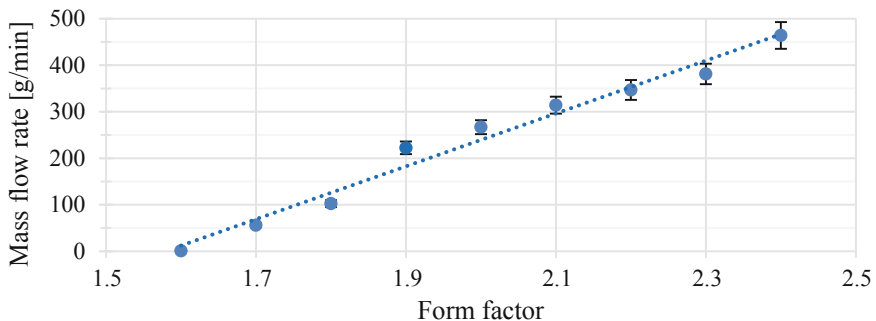

Fig. 19. Mass flow rate with different FF (DL = 35%, LT = 0.15 mm)

The lowest flow rate is to be assigned to a sample from the variation of the form factor (FF = 1.60/pore width = 37 µm) with a value of 0.7 g/min. The lowest value from the variation of the layer thickness (LT = 0.16 mm/ pore width = 22 µm) is 8.7 g/min. It is noticeable that the test specimens show a higher flow rate with smaller pore size when the layer thickness is varied compared to the variation of the form factor. The measurements of the test specimens, produced with a DL of 70%, also show a linear relationship between the FF and the mass flows (r $\geq$ 0.97).
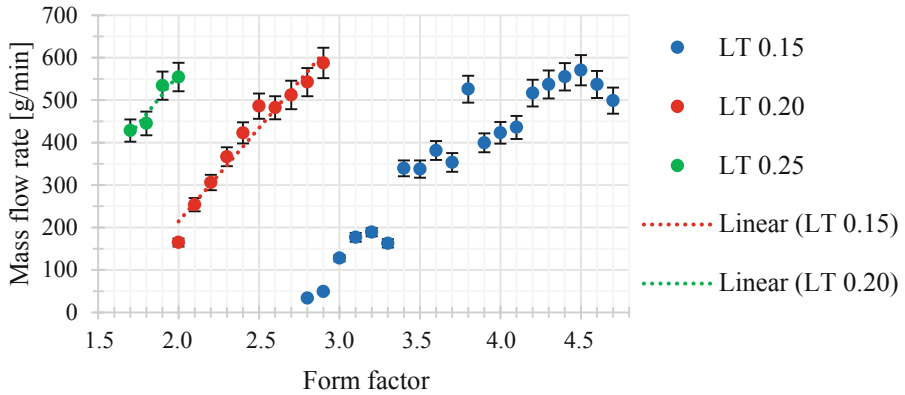
Fig. 20. Mass flow rate with different FF and LT (DL = 105%)

While a linear trend can be seen at LT of 0.25 mm and LT of 0.20 mm (r ≥ 0.96), there is a dispersion of the measured values at LT of 0.15 (see Fig. 20). The combination of the low layer thickness and the too high discharge level does not allow an even and reproducible droplet deposition. This results in an uneven porous structure for which there is no linear trend in liquid permeability. At this point it should be noted that liquid permeability is not only dependent on the size of the pore openings. The free pore volume in the transverse direction of the samples also influences the volume flow. The highest mass flow rate determined is 587.7 g/min (DL = 105%, FF = 2.90, LT = 0.20 mm).

Due to the mainly linear relationships between the process parameters and the resulting mass flows, the permeability coefficients are calculated only for the smallest and largest mass flows. The permeability coefficients are $k_f = 5.09 \times 10^{-3}$ m/s ($\dot{m}$ = 587.7 g/min) and $k_f = 6.06 \times 10^{-6}$ m/s ($\dot{m}$ = 0.7 g/min). According to DIN 18130-1 (see Table 1), components with the following properties can be manufactured:

- Highly permeable
- Permeable
- Low permeability

6 Summary and Outlook

The investigations have shown that it is possible to produce porous structures with the APF process. The free spaces of the components form a lattice structure of open pore channels, which is uniformly structured in horizontal and vertical direction. Due to a connection between the cavities the inner structure is called an "interconnected pore structure". The pore width at the surface of the components is adjustable in the size range 22 to 466 μm and thus belongs to the range of macropores. According to

ISO 4793, this corresponds to laboratory filters of the category P 3 to P 00, which are used for the analytical filtration of medium-fine precipitates or as a support for solid samples in flow systems.

The variable size adjustment results in a porosity between 7 and 66%. When ABS is used, this corresponds to a weight reduction of up to 70%. At the same time, the material savings lead to a cycle time reduction of up to 75%. As a result of the reproducibility tests, a tolerance range of the pore widths of ± 10 µm is specified. This value cannot be transferred to the pore openings on the platform side, as the geometry is influenced by varying degrees of pressure on the droplet strands in the first layer. This influence is so significant that average deviations of the pore widths of -38 µm and $+14$ µm occur. If the geometry or the number of components is varied within a building job, this has no influence on the pore size.

The level of liquid permeability is not directly related to the size of the openings of the surface pores. In addition, the volume flow rate that occurs depends on the selected layer thickness. At constant layer thickness there is a linear relationship between permeability and the parameter form factor. With the manufactured components, permeability coefficients between 5.09×10^{-3} and 6.06×10^{-6} m/s were achieved for the flow of water. In accordance with DIN 18130-1, these values are assigned to the areas of high permeability, permeability and low permeability.

The application possibilities of open-pored structures are numerous. In addition to components already in use, such as compressed air ejectors in injection molds or filters for separating media, research is being conducted into further possible applications. Examples are porous electrode or battery components within accumulators for the automotive sector or new types of structures for use in heat and air exchangers [16]. In addition to the characteristics already investigated, further properties must be tested according to the field of application. One aspect to be investigated is the mechanical strength of the structures. For the application as a filter, the absorption capacity of compressive forces is of particular importance. When a medium flows through the filter, the filter material must be able to resist the pressure applied by the flow.

References

1. Gaub, H.: Customization of mass-produced parts by combining injection molding and additive manufacturing with Industry 4.0 technologies. Reinf. Plast. **60**(6), 401–404 (2016)
2. Neff, M., Kessling, O.: Geschichtete Funktionsteile im industriellen Maßstab. Kunststoffe, Nr. 08/2014, pp. 64–67 (2014)
3. Keßling, O.: AKF - Neues industrielles additivesVerfahren. RTejournal - Forum für Rapid Technologie, vol. 2015. https://www.rtejournal.de/ausgabe11/3963. Accessed 12 Feb 2020
4. Kloke, A: Tröpfchen im Millisekundentakt. Kunststoffe 11/2018. Carl Hanser Verlag, München (2018)
5. Duffner, E.: Industrielle additive Fertigung funktionsfähiger Kunststoffteile. Lightweight Des. **9**, 22–27 (2016)
6. Ramezani Dana, H., Ben Azzouna, M., Breteau, T., Delbreilh, L., Guillet, A., Barbe, F.: Développement de matériaux cellulaires avec mise en oeuvre par fabrication additive bimatière (2017)

7. Hirsch, A., Hecker, F., Moritzer, E.: Process parameter optimization to improve the mechanical properties of Arburg Plastic Freeformed components. In: Conference Proceeding, 30th Annual International Solid Freeform Fabrication Symposium (SFF), Austin, Texas (2019)

8. Kaut, F., Cepus, V., Grellmann, W., Lach, R.: Structure-property relationship of additive manufactured thermoplastic polymers processed with ARBURG Freeformer Technology. Rapid.Tech – Fachkongress, Forum AM Science, pp. 217–235 (2018)

9. Guessasma, S., Nouri, H., Roger, F.: Microstructural and mechanical implications of microscaled assembly in droplet-based multi-material additive manufacturing. Polymers **9**, 372 (2017)

10. Spiller, Q., Müller, T., Plewa, K., Hanemann, T., Fleischer, J.: Eignung des Kunststoff-Freiformens für metallische Bauteile (2016)

11. Klahn, C.: Laseradditiv gefertigte luftdurchlässige Mesostrukturen - Herstellung und Eigenschaften für die Anwendung. Springer, Hamburg (2015)

12. Thienel, K.-Ch.: Werkstoffkunde 1. Lecture script, University of the Bundeswehr, München (2011)

13. Menges, G., Haberstroh, E., Michaeli, W., Schmachtenberg, E.: Menges Werkstoffkunde Kunststoffe, 5th edn. Carl Hanser Fachbuchverlag, Wien (2014)

14. Häfner, F., Wagner, S., Freese, C.: Durchlässigkeitsmessung - Bestimmung der absoluten Durchlässigkeit pröser Stoffe mit Flüssigkeit und Gas. TU Freiburg - Institut für Bohrtechnik und Fluidbergbau, Freiburg (2015)

15. Günther, K., Sonntag, F., Moritzer, E., Hirsch, A., Klotzbach, U., Lasagni, A.F.: Universal Micromachining Platform and Basic Technologies for the Manufacture and Marking of Microphysiological Systems. Micromachines **8**, 246 (2017)

16. Hagl, R.: Das 3D-Druck-Kompendium - Leitfaden für Unternehmen, Berater und Innovationstreiber, 2nd edn. Springer, München (2015)